LETTERS
https://doi.org/10.1038/s41567-020-0791-2
nature physics

Macroscopic patterns of interacting contagions are indistinguishable from social reinforcement

Laurent Hébert-Dufresne[1,2,3]✉, Samuel V. Scarpino[4,5,6,7,8,9] and Jean-Gabriel Young[10]

From 'fake news' to innovative technologies, many contagions spread as complex contagions via a process of social reinforcement, where multiple exposures are distinct from prolonged exposure to a single source[1]. Contrarily, biological agents such as Ebola or measles are typically thought to spread as simple contagions[2]. Here, we demonstrate that these different spreading mechanisms can have indistinguishable population-level dynamics once multiple contagions interact. In the social context, our results highlight the challenge of identifying and quantifying spreading mechanisms, such as social reinforcement[3], in a world where an innumerable number of ideas, memes and behaviours interact. In the biological context, this parallel allows the use of complex contagions to effectively quantify the non-trivial interactions of infectious diseases.

On 27 September 2016, the World Health Organization declared that measles had been eliminated from the Americas[4]. Less than two years later, an outbreak of the disease in Venezuela sparked an epidemic across South America, which is ongoing and has sickened tens-of-thousands[5–7]. Concurrently, the number of measles cases has increased in all but one of the World Health Organization regions[8], over 80,000 cases (with a hospitalization rate > 60%) occurred in the European Union[9], and the United States of America experienced 17 measles outbreaks[5,10]. The majority of these cases occurred in unvaccinated individuals[11–13]. From collapsing public health infrastructure[14] and lack of access to vaccines[7] to non-medical exemptions, for example, religious beliefs[15,16], and the spread of fraudulent science[17–19], the precise reasons individuals go unvaccinated are myriad; however, underlying all of these mechanisms is the coupled transmission of two contagions, one biological and one—or more—social.

Clearly, contagions never occur in a vacuum; instead, pathogens and ideas interact with each other and with externalities such as host connectivity, behaviour and mobility. Nevertheless, many biological contagions are still considered to be 'simple', where infectious individuals transmit to susceptible individuals independently of anything else occurring around the individuals[2]. The term simple contagion is a misnomer, since many epidemic models need to be incredibly complicated to account for the rich diversity of biological pathogens and human behaviours; including non-Markovian dynamics[20], heterogeneous contact structure[21], vector-borne diseases[22] and evolutionary dynamics[23]. Yet, in almost all cases, the probability of a transmission event depends only on the states of the possible infector and infectee. Conversely, in complex contagions, as defined for instance in recent multidisciplinary work[1,24], the spreading mechanism explicitly depends on the context of transmission events, usually via the neighbourhood of the susceptible individuals, such that pairwise information becomes insufficient to model the transmission process[25,26]. For example, social reinforcement can lead to a transmission rate effectively proportional to the number of different infectious contacts to which a susceptible individual is exposed[3]. This mechanistic difference creates a false dichotomy, forcing us to choose the mechanism we think best describes the reality of a given contagion. In practice, the context of transmission events always matters.

When modelling a contagion, the choice of mechanism is critical because simple and complex contagions tend to induce substantially different dynamics and can lead to incompatible conclusions about intervention strategies or risk. An important difference is that complex contagions do not always feature a monotonous relation between the expected epidemic size and their average transmission rate, unlike simple contagions[27,28]. Instead, microscopic variations in transmission rate can lead to macroscopic jumps in expected epidemic size. This effect, that small changes in transmission can lead to large differences in outbreak size, occurs because the population effectively builds up a latent epidemic potential[29] where many individuals would infect their susceptible neighbours if only a few of them had one more infectious neighbour. Eventually, often due only to small variations in initial conditions or transmission rate, a macroscopic cascade of infections that releases this latent epidemic potential will occur. The importance of correlations between the states of neighbours also explains why complex contagions can benefit from network clustering (that is triangles), again unlike simple contagions[30].

Several models have been developed to study interacting contagions, often to investigate how the spread of awareness might slow an infectious disease through a duelling contagion framework[31–34]. These models are often limited to two interacting contagions since, as we will see, the required number of parameters and assumptions grows exponentially with the number of considered contagions. Despite their complicated structure, these studies have provided several useful insights. Importantly, it was shown that positively interacting contagions feature discontinuous phase transitions and can benefit from network clustering[35]. Consider for example the interaction between influenza and other respiratory pathogens—for example, *Streptococcus pneumoniae*, rhinoviruses, adenovirus and so on—which can interact in different ways: an individual with a compromised immune system due to one infection might be more susceptible to the other, or an individual with both infections might exhibit heightened symptoms and increased transmission rates[36–39].

[1]Department of Computer Science, University of Vermont, Burlington, VT, USA. [2]Vermont Complex Systems Center, University of Vermont, Burlington, VT, USA. [3]Département de Physique, de Génie Physique et d'Optique, Université Laval, Quebec City, Quebec, Canada. [4]Network Science Institute, Northeastern University, Boston, MA, USA. [5]Marine & Environmental Sciences, Northeastern University, Boston, MA, USA. [6]Physics, Northeastern University, Boston, MA, USA. [7]Health Sciences, Northeastern University, Boston, MA, USA. [8]Dharma Platform, Washington, DC, USA. [9]ISI Foundation, Turin, Italy. [10]Center for the Study of Complex Systems, University of Michigan, Ann Arbor, MI, USA. ✉e-mail: laurent.hebert-dufresne@uvm.edu

Box 1 | Well-mixed compartmental SIS models

We use the simple SIS process to highlight the mathematical mapping between complex contagions and interacting simple contagions. In the SIS process, infectious individuals infect susceptible individuals, but also recover back to the susceptible state. A general complex contagion model can be followed using an ordinary differential equation for the density $I(t)$ of infectious individuals at time t. Omitting the obvious temporal dependency, we write

$$\dot{I} = \beta(I) I (1 - I) - \gamma I \tag{1}$$

where γ is the recovery rate and $\beta(I)$ describes the transmission rate per contact given that there is a density $I(t)$ of infectious individuals in the population. For example, an increasing $\beta(I)$ can describe a social reinforcement mechanism.

We can write similar equations for two interacting simple contagions by tracking the density $[SS]$ of individuals that are susceptible to both contagions, the densities $[IS]$ and $[SI]$ that are infected by the first or second contagion alone, and the density $[II]$ that are co-infected. We are mostly interested in the density of nodes $\tilde{I} = [IS] + [II]$ that are infected by the first contagion. We therefore follow

$$\begin{aligned}[\dot{II}] = {} & [IS](\beta_2[SI] + \alpha\beta_2[II]) \\ & + [SI](\beta_1[IS] + \alpha\beta_1[II]) - (\gamma_1 + \gamma_2)[II]\end{aligned} \tag{2}$$

$$\begin{aligned}[\dot{IS}] = {} & [SS](\beta_1[IS] + \alpha\beta_1[II]) \\ & + \gamma_2[II] - \gamma_1[IS] - [IS](\beta_2[SI] + \alpha\beta_2[II])\end{aligned} \tag{3}$$

Comparing the sum of equations (2) and (3) with equation (1) shows that the two models are equivalent under the mapping

$$\beta(I) \equiv \beta(\tilde{I}) = \frac{\beta_1[IS] + \alpha\beta_1[II]}{[IS] + [II]} \tag{4}$$

which is a valid mapping from interacting contagions to a complex contagion, for every monotonous form of $[IS] + [II]$ (the vast majority of possible SIS curves). A similar mapping can be obtained for SIR dynamics using the monotonicity of the recovered curve assuming that recovered individuals are now immune.

A population can then build up a latent epidemic potential where many individuals would infect their susceptible neighbours if only a few of them were compromised by a second disease. Therefore, it might not be surprising that interacting contagions can also exhibit macroscopic jumps in expected epidemic size under microscopic variation in the average transmission rates, and that interacting contagions can also benefit from network clustering. Even for single pathogens spreading through a population, if different routes of transmission have drastically different transmission probabilities (for example, human immunodeficiency virus sexual transmission versus transmission through needle sharing[40,41] or Zika sexual transmission from men versus women[42]), they will spread more like complex contagions.

Here, we demonstrate that the connection between complex and interacting contagions runs far deeper than shared phenomenology. In Box 1, we present simple models of interacting and complex contagions in well-mixed populations and demonstrate that there exists an exact mapping between the two models; that is, the simple model with interactions can always be expressed as a complex contagion. Figure 1 summarizes the interesting dynamical features of these models, namely their potential for discontinuous jumps in expected epidemic size as well as regimes of faster than exponential spread. Figure 1 also highlights the mathematical mapping between the two dynamics. Every curve of Fig. 1 can be obtained by solving the differential equations for either interacting or complex contagions. The solutions are identical. Consequently, it follows that in any context where the assumption of a well-mixed population holds, interacting contagion models are indistinguishable from complex contagions—provided we are unaware of potential interactions among pathogens, and are not collecting the corresponding co-infection data. Given that both assumptions, well-mixed populations and data from a single pathogen, are often considered to hold in contained environments such as schools, workplaces and homogeneous social groups[43], our results demonstrate that, unless the process follows strictly simple dynamics, even perfect incidence data for a single contagion in these environments cannot be used to identify the true spreading mechanism.

The situation is different in a heterogeneous environment, where contagions follow some underlying contact network. In this context, a contagion process is not fully described by simply following the number of infections in time, and the identity and contacts of infected individuals matter for the dynamics. The authors of a recent study leveraged this idea to study memes by quantifying their spread within and across communities[25]. Their approach is based on the fact that for complex contagions, unlike simple contagions, "the spread within highly clustered communities is enhanced, while diffusion across communities is hampered". They identify a number of statistics that can help distinguish simple and complex contagions (for example, the number of early adopters of memes (number of contagious nodes at early times) and the state of their neighbours). The logic is that if contagions benefit from network clustering, states of neighbours should be more correlated than expected from the network structure alone.

Unfortunately, interacting contagions also benefit from network clustering in similar ways[35], which can lead us to confuse the two. Using simulations on a known contact network, we find that looking for state correlations between neighbours can indeed distinguish interacting and complex contagions from simple contagions as previously claimed[25]. However, we also find that this method cannot distinguish complex and interacting contagions from one another.

In our experiments, we simulate simple, interacting and complex contagions on both regular random contact networks with 20 random contacts for every node and equivalent but clustered networks where nodes now belong to cliques of size 12 (11 contacts per node within cliques) and have 9 additional random contacts (see Fig. 2). We use these regular networks to avoid confounding the effect of clustering with that of assortativity[35] and to reduce noise in the observed statistics. We increase the transmission rates of both contagions by a factor of 7 when they appear on the same contact—this interaction parameter might appear high but is actually far from, for example, the interaction factor between influenza and pneumococcal pneumonia, which can be up to 100-fold[44]. The results of these simulations are straightforward (Fig. 2): when parametrized correctly such that all three contagion models can reach the same level of prevalence after some desired time period, we find that interacting and complex contagions can be easily distinguished from simple contagions, but not from one another. This shows not only that non-simple contagions benefit from clustering in network structure, but also that this clustering can lead to similar increases in statistical correlations between cases for different contagion mechanisms.

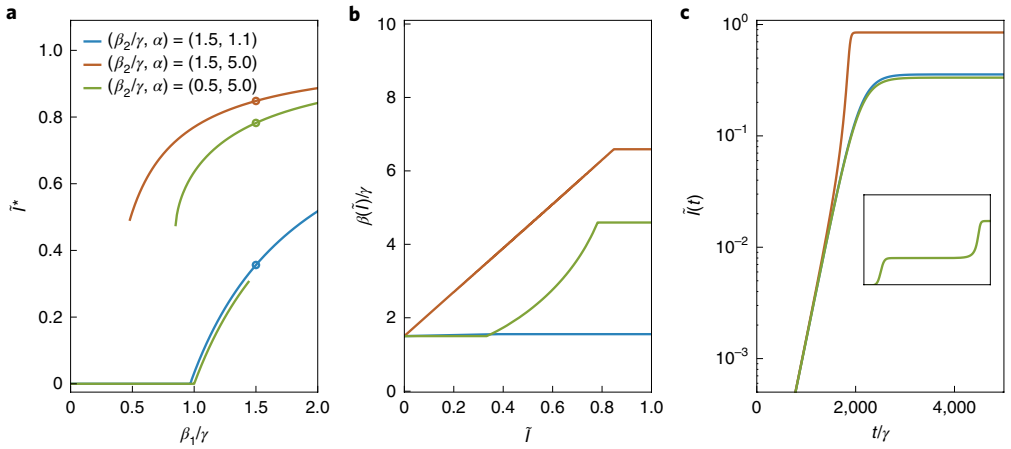

Fig. 1 | Analytical solutions of both susceptible–infectious–susceptible (SIS) ordinary differential equation systems from Box 1 for both interacting simple contagions and complex contagions. a, The expected final epidemic size, which can undergo a continuous, hybrid or discontinuous transition at varied epidemic thresholds. All contagions use the same recovery rate, $\gamma_1 = \gamma_2 = \gamma$, while other parameters are specified in the figure. We highlight three parameter sets (circled) whose full behaviour is explored in **b** and **c**. **b**, The effective transmission rate per infectious contact, which is monotonously increasing in all cases. In the continuous transition regime (blue curve), $\beta(\tilde{I})$ is almost but not quite constant at β_1. In the hybrid transition regime (green curve), β_1 is flat until $\tilde{I}$ reaches the expected epidemic size $\tilde{I}^*$ of its second epidemic transition, at which point the synergistic interactions start. In the discontinuous transition regime (orange curve), $\beta(\tilde{I})$ is a linear function of $\tilde{I}$. **c**, The varied time evolution of $\tilde{I}(t)$. In the continuous regime (blue curve), we see exponential growth with saturation at equilibrium. In the discontinuous regime (orange curve), we see exponential growth followed by a regime of rapid acceleration. In the hybrid regime (green curve), we see both behaviours in an evolution with two plateaux; mostly visible on the inset, which shows the longer, complete time evolution. All results were obtained both by integrating equations (2) and (3), and by using the obtained $\beta(\tilde{I})$ curve as an input to equation (1). We found that the two approaches, interacting simple contagions or complex contagions, give exactly the same results in all regimes.

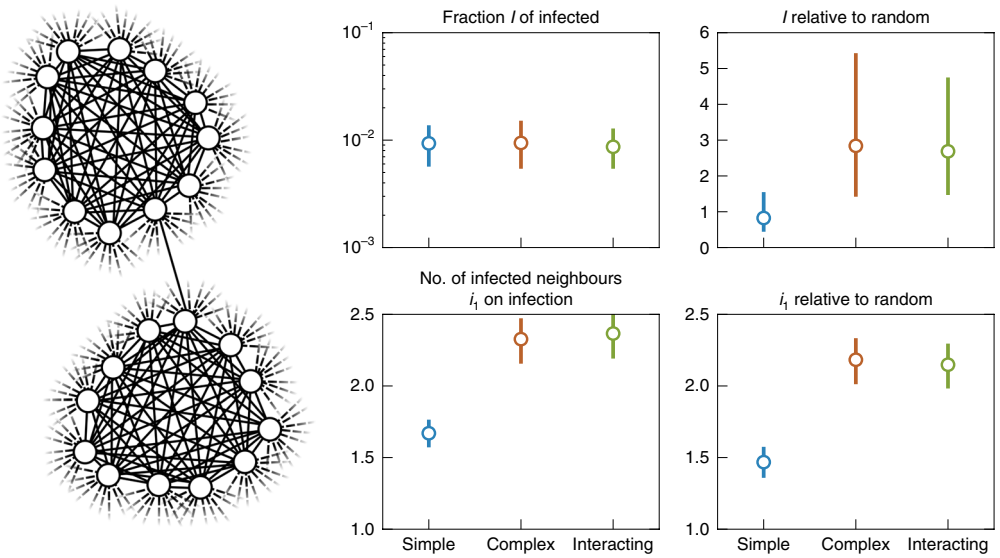

Fig. 2 | Statistics of SIS simulations of simple, interacting and complex contagions. Left: the contact network structure used in the simulations. All 10^4 nodes belong to a single clique of size 12 and have an additional 9 random neighbours, for a global clustering coefficient $C = 0.29$. Right: the observed phenomenology. The fraction of infected nodes after 5,000 time steps and the average number of infectious neighbours following infection of a node, as well as a comparison of the same features versus expectations on an equivalent random network (same degree distribution, but all edges are uniformly randomized). We show the median value of all statistics as well as their 50% confidence interval. Parameters were chosen such that the fraction of infected nodes are similar after the 5,000 time steps. The simple contagion uses a transmission probability of 8×10^{-5} and a recovery probability of 10^{-3}. The interacting simple contagions use a transmission probability of 12×10^{-6} and a recovery probability of 10^{-3}, but the transmission probability increases by a factor of 15 if the other disease is present on the contact (in either the susceptible or infectious node) and the recovery probability decreases by a factor of 2 and 3 for the first and second disease if a node is infected by both. The statistics shown are for the first disease alone. Finally, the complex contagion uses transmission and recovery probability that depend on the number k of infectious neighbours. The transmission probability follows a sigmoid $p_0 + (3/4)p_0/(1 + \exp(-2(k-2))$ with $p_0 = 5 \times 10^{-5}$ whereas the recovery probability simply falls as $10^{-3}/k$.

Altogether, the results from Box 1 and Figs. 1 and 2 show that complex contagions and interacting simple contagions possess the same dynamical and statistical features, even if the mechanisms behind both models are completely different. Since we know real-world pathogens can interact with unknown numbers of other pathogens—or different strains/serotypes of the same pathogen—the

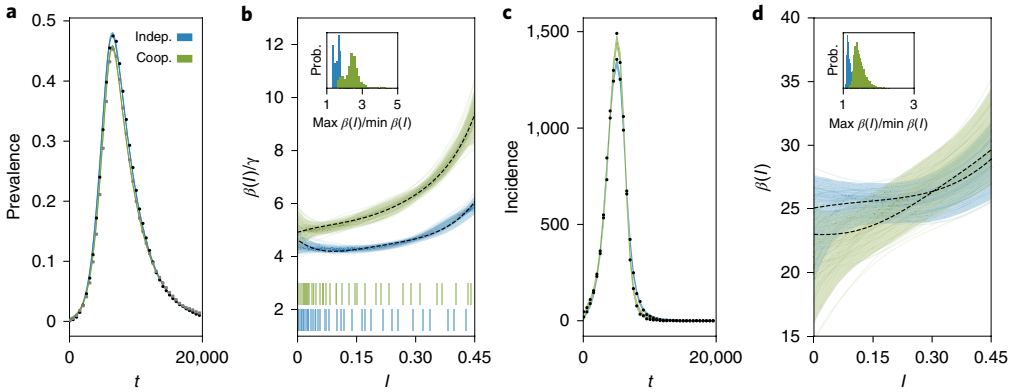

Fig. 3 | Signatures of non-interacting and interacting SIR epidemics. We simulate the SIR process in the case of non-interacting and interacting simple contagions on clustered contact networks where each of 10,000 individuals belongs to 2 cliques of size 5. **a**,**c**, The dynamics of the density of infected individuals for epidemics taking place on the same networks (**a**), and the corresponding incidence time series (**c**). Parameters were chosen to produce roughly similar time series. In one case (blue data), two diseases with a transmission rate of 3/10 and a recovery rate of 1/3 spread without interaction, and we show the evolution of only one of them. In the other case (green data), two diseases with a transmission rate of 1/10 and a recovery rate of 1 interact positively by increasing their transmission rate by a factor of 7 whenever the other disease occurs on the same contact and decreasing their recovery rate by the same factor when an individual is co-infected. We again show the evolution of only one of the two diseases. The coloured curves are Bayesian fits of a continuous model of complex contagion in a well-mixed population[51]; the simulated time series are shown with small filled symbols. **b**, The inferred complex contagion function $\beta(I)/\gamma$ for the two series from prevalence data, with the density of observations illustrated with bar plots below. The maximum a posteriori fit is shown with a dotted line, with the 5th to 95th percentiles (shaded region), and 100 randomly selected posterior samples (coloured transparent lines) that highlight the sample-to-sample variability. The insets describe how close the inferred transmission functions are to a flat transmission rate by plotting the distribution of the ratio of the maximal to minimal values in the posterior samples. In both cases, the transmission functions inferred on the time series of interacting contagions are significantly different from the transmission functions inferred on non-interacting contagion data. **d**, The same inference, but from incidence data.

logical conclusion is that we ought to model real contagions as complex contagions. Critically, these contagions need not all be biological and pathogens can interact with, for example, the spread of a behaviour. Additionally, simple contagions dynamics are a subset of the complex contagion model, meaning that if the pathogen does not interact with other contagions, the model can recapitulate its dynamics. More importantly, by using the complex contagion model, we avoid the need to procure exponentially more data and estimate exponentially more model parameters as the number of interacting contagions increases; instead we can use a general parametrization to find a complex transmission function $\beta(I)$ governing the effective infection rate for every pathogen of interest.

We thus develop a framework to infer a function $\beta(I)$ that reproduces some contagion time series from a complex contagion Markov model of susceptible–infectious–recovered (SIR) dynamics[2]. Essentially, this is the same well-mixed model as shown in Box 1 but where individuals who recover are now immune to the contagion instead of returning to the susceptible state. As most real contagion data tend to be non-monotonous (that is, they have a growth period, a peak and a period of decay), the SIR model is probably more appropriate for empirical data. In this framework, we inverse the differential equations to infer a $\beta(I)$ function from data by assuming some Gaussian noise around the deterministic $I(t)$ equation and using a parametrization of $\beta(I)$ in terms of Bernstein polynomials (a detailed description is given in the Supplementary Information).

Our procedure focuses on $\beta(I)$ instead of an instantaneous transmission rate $\beta(t)$ as used previously[45] for two reasons. First, using $\beta(I)$ instead of an instantaneous $\beta(t)$ avoids overfitting to noise in the instantaneous growth rate of a time series $I(t)$, since we combine the information contained in both the rise and fall of a contagion. Second, using $\beta(I)$ maps real data to well-studied Markovian (that is, memory-less) complex contagions and therefore also provides an easy way to compare contagions independently of time and initial conditions. Last, we provide a formulation of the inference procedure for both prevalence (current infectious cases) and incidence data (new cases per unit time) in the Supplementary Information.

We illustrate the value of this inference procedure on simulations of both interacting and non-interacting simple contagions in Fig. 3. We selected parameter values to produce two very similar time series to test our framework on a hard instance of the contagion inference problem. While the only noise in the data is that of the regular stochasticity of epidemic simulations, we used a relatively low sampling rate and used a single realization of both interacting and non-interacting contagion processes. Even in this context, we find that the strength of the interaction is reflected in how much the inferred $\beta(I)$ function deviates from a simple constant transmission rate, as measured by the ratio of the maximal to minimal values in the inferred $\beta(I)$ function. One advantage of using the inferred $\beta(I)$ function is that it highlights features of a contagion not readily visible in its time series alone, such as the velocity of the contagion, which is not restricted to exponential spread unlike classic models. Our results therefore showcase how a robust framework of complex contagion can be used to quantify interactions or simply distinguish and classify contagions.

To illustrate the potential of our framework for real-world contagions, we can infer the presence of complex contagion dynamics in a wide range of contagion data. In doing so, we identified a few interesting cases that go against the conventional wisdom that biological pathogens spread as simple contagions while social pathogens spread as complex contagions through social reinforcement. First, we focus on social pathogens, namely memes and news, to find cases where loss of novelty of the pathogen, or depletion of susceptibles, decreases its transmission rate (that is, $\mathrm{d}\beta/\mathrm{d}I < 0 \,\forall\, I$) contrarily to most other social contagions. We show one such case in Fig. 4a, using the incidence of news and social media posts related to Walter Cronkite's death in 2009. Nevertheless, recent work on collective attention dynamics on social media finds evidence that meme spreading is—as expected—often characterized by accelerating rates of spreading[46]. Our results provide a general explanation

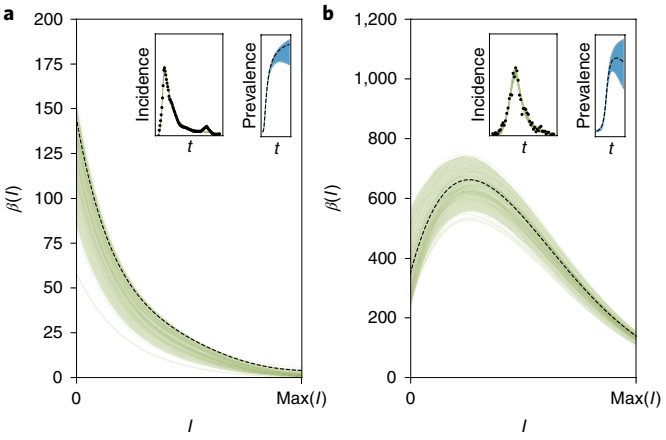

Fig. 4 | Complexity of real social and epidemiological contagions. We fit the time series shown in the insets—the empirical incidence of two real complex contagions—using the SIR version of our model. **a**, A series depicting the number of mentions of Walter Cronkite's death on social media[52]. **b**, The overall incidence for the 2005 dengue outbreak in Puerto Rico[53]. The main plots show the posterior distribution and maximum a posteriori estimate for the contagion function. The maximum a posteriori fit is shown with a dotted line, with the 5th to 95th percentiles (shaded region), and 100 randomly selected posterior samples (coloured transparent lines) that highlight the sample-to-sample variability. Note that the prevalence (second insets, in blue) is not actually observed. Both contagions slow down as the infected density increases, one from the start (social contagion), and the other after a rapid initial acceleration (dengue).

for why such dynamics are expected to occur often in social contagions, but can still account for 'contagions' where novelty causes a decrease in transmission rate (for example, the previous example of Walter Cronkite's death).

Second, we pick a biological contagion with known interactions: dengue virus. Indeed, there are well-documented interactions across dengue strains based on antibody-dependent enhancement[47,48]. In this interaction mechanism, antibodies from a primary dengue infection bind to dengue virus particles of a different serotype, which does not neutralize virus particles and in fact helps them infect cells. To illustrate the utility of our inference methodology, we focus on the 2005 dengue outbreak in Puerto Rico—as it features a combination of two dengue strains (DENV 2 and 3)—and, as expected from our previous simulations, we find a significant increase in the transmission rate from the onset of the outbreak to about half of its peak value. Surprisingly, the inferred transmission function is non-monotonous and then declines around peak incidence; potentially due to the depletion of more susceptible individuals (see Supplementary Information).

Future work should focus on leveraging our effective, complex contagion model to more broadly uncover known and unknown interactions across infectious diseases and social contagions. For example, with data on co-infections by dengue serotype, we could test the model's ability to distinguish between multi- and single-strain dengue virus outbreaks using only aggregate data. After demonstrating the utility of our model to distinguish dengue outbreaks, one could attempt to quantify unknown biological interactions between various infectious diseases. In doing so, one must take care to correctly assess the impact of varied network structures[45] and different model mechanisms including: spontaneous infections[49], disease vectors[22] or multiple exposures[50]. In addition, our complex contagion model—paired with high-resolution epidemiological data—can be used to search for the presence of complex, biological contagions (that is, single pathogen systems where the probability of infection is a nonlinear function of the number of exposures).

In summary, interacting simple contagions are mathematically equivalent to complex contagions if we assume well-mixed populations. Furthermore, even if we know the underlying contact network, previously proposed statistics—such as the number of infectious neighbours following infection or recovery—mostly help to distinguish complex contagions or interacting contagions from simple contagions, but not necessarily from one another. That we are unable to distinguish interacting contagions from complex contagions on networks using these statistics suggests that their physical equivalence can be proved even in the absence of mass action mixing. Unfortunately, this non-identifiability also implies that phenomenology and model fitting cannot identify or quantify spreading mechanisms if we are not fully aware of all possible interactions and co-infections. One consequence is that measurements of complex spreading mechanisms, such as social reinforcement, might be practically impossible unless one can explicitly control for unknown interactions. Otherwise, observations of the spread of an individual meme or biological contagion in a real social system will always be confounded by the innumerable number of ideas, pathogens and behaviours that might be interacting with each other and with the contagion. Even worse, in practice we rarely have a perfect knowledge of the underlying contact network, such that the variations in transmission rate due to interactions are also combined with variations due to the unknown contact structure.

We therefore suggest embracing complex contagions as scientifically meaningful, even in the context where one believes the underlying mechanisms are not complex (that is, the complex contagion model can be falsified with experiments). In fact, we claim that, even when social reinforcement and/or nonlinear infection rates have little mechanistic support, complex contagions remain a general, effective framework for contagions of all natures.

Online content

Any methods, additional references, Nature Research reporting summaries, source data, extended data, supplementary information, acknowledgements, peer review information; details of author contributions and competing interests; and statements of data and code availability are available at https://doi.org/10.1038/s41567-020-0791-2.

Received: 1 July 2019; Accepted: 7 January 2020;
Published online: 24 February 2020

References

1. Lehmann S. and Ahn Y.-Y. *Complex Spreading Phenomena in Social Systems* (Springer, 2018).
2. Anderson R. M. and May R. M. *Infectious Diseases of Humans: Dynamics and Control* (Oxford Univ. Press, 1992).
3. Centola, D. The spread of behavior in an online social network experiment. *Science* **329**, 1194–1197 (2010).
4. *Plan of Action for Maintaining Measles, Rubella, and Congenital Rubella Syndrome Elimination in the Region of the Americas: Final Report* (PAHO, 2016); http://www.paho.org/hq/index.php?option=com_docman&task=doc_download&gid=35681&Itemid=270&lang=en
5. Dabbagh, A. et al. Progress toward regional measles elimination worldwide, 2000–2017. *Morb. Mortal. Wkly Rep.* **67**, 1323 (2018).
6. Fraser, B. Measles outbreak in the Americas. *Lancet* **392**, 373 (2018).
7. Elidio, G. A. et al. Measles outbreak: preliminary report on a case series of the first 8,070 suspected cases, Manaus, Amazonas state, Brazil, February to November 2018. *Eurosurveillance* **24**, 1800663 (2019).
8. Friedrich, M. Measles cases rise around the globe. *J. Am. Med. Assoc.* **321**, 238–238 (2019).
9. Thornton, J. Measles cases in Europe tripled from 2017 to 2018. *Br. Med. J.* **364**, 1634 (2019).
10. *Measles Cases and Outbreaks* (US CDC, accessed 18 February 2019); https://www.cdc.gov/measles/cases-outbreaks.html
11. Majumder, M. S., Cohn, E. L., Mekaru, S. R., Huston, J. E. & Brownstein, J. S. Substandard vaccination compliance and the 2015 measles outbreak. *J. Am. Med. Assoc. Pediatr.* **169**, 494–495 (2015).

12. Phadke, V. K., Bednarczyk, R. A., Salmon, D. A. & Omer, S. B. Association between vaccine refusal and vaccine-preventable diseases in the United States: a review of measles and pertussis. *J. Am. Med. Assoc.* **315**, 1149–1158 (2016).
13. Melegaro, A. Measles vaccination: no time to rest. *Lancet Glob. Health* **7**, e282–e283 (2019).
14. Paniz-Mondolfi, A. et al. Resurgence of vaccine-preventable diseases in Venezuela as a regional public health threat in the Americas. *Emerg. Infect. Dis.* **25**, 625–632 (2019).
15. Salmon, D. A. et al. Health consequences of religious and philosophical exemptions from immunization laws: individual and societal risk of measles. *J. Am. Med. Assoc.* **282**, 47–53 (1999).
16. Papachrisanthou, M. M. & Davis, R. L. The resurgence of measles, mumps, and pertussis. *J. Nurse Pract.* **15**, 391–395 (2019).
17. McHale, P., Keenan, A. & Ghebrehewet, S. Reasons for measles cases not being vaccinated with MMR: investigation into parents' and carers' views following a large measles outbreak. *Epidemiol. Infect.* **144**, 870–875 (2016).
18. Sansonetti, P. J. Measles 2018: a tale of two anniversaries. *EMBO Mol. Med.* **10**, e9176 (2018).
19. Mavragani, A. & Ochoa, G. The Internet and the anti-vaccine movement: tracking the 2017 EU measles outbreak. *Big Data Cogn. Comput.* **2**, 2 (2018).
20. Van Mieghem, P. & Van de Bovenkamp, R. Non-Markovian infection spread dramatically alters the susceptible–infected–susceptible epidemic threshold in networks. *Phys. Rev. Lett.* **110**, 108701 (2013).
21. Pastor-Satorras, R., Castellano, C. & Van Mieghem, P. Epidemic processes in complex networks. *Rev. Mod. Phys.* **87**, 925 (2015).
22. Ross R. *The Prevention of Malaria* (Dutton, 1910).
23. Lipsitch, M., Cohen, T., Murray, M. & Levin, B. R. Antiviral resistance and the control of pandemic influenza. *PLoS Med.* **4**, e15 (2007).
24. Centola, D. & Macy, M. Complex contagions and the weakness of long ties. *Am. J. Sociol.* **113**, 702–734 (2007).
25. Weng, L., Menczer, F. & Ahn, Y.-Y. Virality prediction and community structure in social networks. *Sci. Rep.* **3**, 2522 (2013).
26. Mønsted, B., Sapieżyński, P., Ferrara, E. & Lehmann, S. Evidence of complex contagion of information in social media: an experiment using Twitter bots. *PloS ONE* **12**, e0184148 (2017).
27. Liu, W.-m, Levin, S. A. & Iwasa, Y. Influence of nonlinear incidence rates upon the behavior of SIRS epidemiological models. *J. Math. Biol.* **23**, 187–204 (1986).
28. Dodds, P. S. & Watts, D. J. Universal behavior in a generalized model of contagion. *Phys. Rev. Lett.* **92**, 218701 (2004).
29. Hébert-Dufresne, L., Patterson-Lomba, O., Goerg, G. M. & Althouse, B. M. Pathogen mutation modeled by competition between site and bond percolation. *Phys. Rev. Lett.* **110**, 108103 (2013).
30. O'Sullivan, D. J., O'Keeffe, G. J., Fennell, P. G. & Gleeson, J. P. Mathematical modeling of complex contagion on clustered networks. *Front. Phys.* **3**, 71 (2015).
31. Funk, S. & Jansen, V. A. Interacting epidemics on overlay networks. *Phys. Rev. E* **81**, 036118 (2010).
32. Marceau, V., Noël, P.-A., Hébert-Dufresne, L., Allard, A. & Dubé, L. J. Modeling the dynamical interaction between epidemics on overlay networks. *Phys. Rev. E* **84**, 026105 (2011).
33. Bauch, C. T. & Galvani, A. P. Social factors in epidemiology. *Science* **342**, 47–49 (2013).
34. Fu, F., Christakis, N. A. & Fowler, J. H. Dueling biological and social contagions. *Sci. Rep.* **7**, 43634 (2017).
35. Hébert-Dufresne, L. & Althouse, B. M. Complex dynamics of synergistic coinfections on realistically clustered networks. *Proc. Natl Acad. Sci. USA* **112**, 10551–10556 (2015).
36. Morens, D. M., Taubenberger, J. K. & Fauci, A. S. Predominant role of bacterial pneumonia as a cause of death in pandemic influenza: implications for pandemic influenza preparedness. *J. Infect. Dis.* **198**, 962–970 (2008).
37. Althouse, B. et al. Identifying transmission routes of *Streptococcus pneumoniae* and sources of acquisitions in high transmission communities. *Epidemiol. Infect.* **145**, 2750–2758 (2017).
38. Nickbakhsh, S. et al. Virus–virus interactions impact the population dynamics of influenza and the common cold. *Proc. Natl Acad. Sci. USA* **116**, 27142–27150 (2019).
39. Mair, C. et al. Estimation of temporal covariances in pathogen dynamics using Bayesian multivariate autoregressive models. *PLoS Comput. Biol.* **15**, e1007492 (2019).
40. Strathdee, S. A. & Stockman, J. K. Epidemiology of HIV among injecting and noninjecting drug users: current trends and implications for interventions. *Curr. HIV/AIDS Rep.* **7**, 99–106 (2010).
41. Volz, E., Frost, S. D., Rothenberg, R. & Meyers, L. A. Epidemiological bridging by injection drug use drives an early HIV epidemic. *Epidemics* **2**, 155–164 (2010).
42. Allard, A., Althouse, B. M., Scarpino, S. V. & Hébert-Dufresne, L. Asymmetric percolation drives a double transition in sexual contact networks. *Proc. Natl Acad. Sci. USA* **114**, 8969–8973 (2017).
43. Wearing, H. J., Rohani, P. & Keeling, M. J. Appropriate models for the management of infectious diseases. *PLoS Med.* **2**, e174 (2005).
44. Shrestha, S. et al. Identifying the interaction between influenza and pneumococcal pneumonia using incidence data. *Sci. Transl. Med.* **5**, 191ra84–191ra84 (2013).
45. Liu, Q.-H. et al. Measurability of the epidemic reproduction number in data-driven contact networks. *Proc. Natl Acad. Sci. USA* **115**, 12680–12685 (2018).
46. Lorenz-Spreen, P., Mønsted, B. M., Hövel, P. & Lehmann, S. Accelerating dynamics of collective attention. *Nat. Commun.* **10**, 1759 (2019).
47. Halstead, S. Antibody-enhanced dengue virus infection in primate leukocytes. *Nature* **265**, 739 (1977).
48. Halstead, S. B. Neutralization and antibody-dependent enhancement of dengue viruses. *Adv. Virus Res.* **60**, 421–467 (2003).
49. Hill, A. L., Rand, D. G., Nowak, M. A. & Christakis, N. A. Emotions as infectious diseases in a large social network: the SISa model. *Proc. R. Soc. B* **277**, 3827–3835 (2010).
50. Janssen, H.-K., Müller, M. & Stenull, O. Generalized epidemic process and tricritical dynamic percolation. *Phys. Rev. E* **70**, 026114 (2004).
51. Carpenter, B. et al. Stan: A probabilistic programming language. *J. Stat. Softw.* https://doi.org/10.18637/jss.v076.i01 (2017).
52. Yang, J. & Leskovec, J. Patterns of temporal variation in online media. In *Proc. 4th ACM International Conference on Web Search and Data Mining* (eds King, I. & Li, H.) 177–186 (ACM, 2011).
53. *Dengue Forecasting Project* (NOAA, accessed 10 March 2019); https://dengueforecasting.noaa.gov/

Data availability

The data represented in Figs. 1–4 are available as Source Data. Raw data and processing scripts are available online (https://github.com/jg-you/complex-coinfection-inference/; https://github.com/Emergent-Epidemics/Puerto_Rico_Arbovirus_Data).

Code availability

The inference software is available online (https://github.com/jg-you/complex-coinfection-inference/).

Acknowledgements

L.H.-D. acknowledges support from the National Science Foundation grant DMS-1829826 and the National Institutes of Health 1P20 GM125498-01 Centers of Biomedical Research Excellence Award. S.V.S. acknowledges support from start-up funds provided by Northeastern University. J.-G.Y. is supported by a James S. McDonnell Postdoctoral Fellowship. We also thank A. Allard, B. M. Althouse, M. Newman, G. Cantwell and A. Kirkley for insightful discussions as well as J. Burkardt for sharing his Bernstein polynomial implementation.

Author contributions

L.H.-D. conceived the study and conducted the simulations. J.-G.Y. designed and implemented the inference procedure. L.H.-D. and J.-G.Y. performed the calculations. S.V.S. compiled the empirical data. All authors interpreted the results and wrote the manuscript.

Competing interests

The authors declare no competing interests.

Additional information

Supplementary information is available for this paper at https://doi.org/10.1038/s41567-020-0791-2.

Correspondence and requests for materials should be addressed to L.H.-D.

Peer review information *Nature Physics* thanks Nicholas Christakis and the other, anonymous, reviewer(s) for their contribution to the peer review of this work.

Reprints and permissions information is available at www.nature.com/reprints.